

An update to the Grabinsky et al. (2021) plug strength method

Murray Grabinsky ^{a,*}, Mohammadamin Jafari ^a, Ben Thompson ^a

^a Paterson & Cooke, Canada

Abstract

A common backfilling strategy for tall (e.g. longhole) open stopes is to pour in 2 stages, i.e. to first pour a ‘plug’ of backfill to a few metres above the undercut’s brow, followed by a ‘main’ backfill pour after a suitable cure period. The purpose of the plug is to gain sufficient strength to protect the backfill containment structure in the undercut from the additional stresses due to the main pour. Grabinsky et al. (2021) proposed an analysis method based on a failure mechanism motivated by the Prandtl approach to design structural footings in clays. The method was numerically calibrated and then verified using 4 case studies (3 continuous pours, and one staged pour) in heavily instrumented stopes with complementary strength data from field and laboratory experiments. The authors have used the method extensively to define plug strength for two-stage pouring strategies. They are also aware that the method has been applied by others for a wide range of mining conditions, many of which do not strictly conform to the original assumptions. Therefore, enhancements and extensions to the original method need to be considered.

Sound justification now exists for the assumption that cohesion, $c = \frac{1}{2}UCS$. For draining backfill (i.e. hydraulic fill) friction can also be accounted for which significantly stabilises the backfill plugs. It is not recommended that the plug strength method be applied to waste rock berms, and some alternate plug design criteria are suggested. Irregular geometric effects are addressed, including a new shape factor to be used when rectangular (versus square) undercut drift cross-sections are encountered. Transitional geometry between the undercut and main stope is shown to not have any additional stabilising effect. These changes significantly expand the scope of application for the plug strength method. While these improvements provide increased efficiency, the inherent conservatism of the design approach is reduced, and so it is therefore necessary to consider an appropriate strength factor. Instrumentation is also recommended as necessary to verify plug strength assumptions as part of any design application.

Keywords: cemented paste backfill, plug strength, two-stage pour

1 Introduction

Backfilling tall open stopes is often completed in at least 2 stages with the first backfilling stage being called a ‘plug pour’ followed by a second ‘main pour’ backfilling stage. The purpose of the plug backfill is to cure and achieve a prescribed minimum strength to protect the containment barricade from the additional loading affect arising from main backfilling. In this way, the barricade only needs to be designed for a worst-case scenario of backfill fluid head acting equivalent to the plug depth. A second plug design metric is a requirement for paste strength to be sufficient to prevent liquefaction of the backfill. Liquefaction considerations are addressed in Grabinsky et al. (2025, 2026), while this paper focuses on recent developments in analysis techniques used to assess the required plug strength.

Plug design was originally empirical. For example the Australian Centre for Geomechanics’ 2005 *Handbook on Minefill* (Potvin et al. 2005) suggests pouring the plug to a few metres above the undercut brow and allowing it to cure to 150 kPa (the strength reference presumably referring to the plug backfill’s unconfined

* Corresponding author. Email address: murray.grabinsky@patersoncooke.com

compressive strength [UCS], although it's unclear where this strength is to be realised: i.e. plug mid-height or top plug layer). However, the rationale for this recommendation was not revealed.

The first publication to propose an analysis method in support of rational plug strength design was by Grabinsky et al. (2021). The proposed analytic solution was motivated by the Prandtl solution for punch indentation in a perfectly plastic material, as explained by Skempton (1951) and applied with modifications for assessing the bearing capacity of shallow footings founded on undrained clay. There are inherent restrictions in terms of material property assumptions and geometric assumptions, for both the Skempton (1951) bearing capacity solution and the subsequent Grabinsky et al. (2021) plug strength solution. Regardless, the Grabinsky et al. (2021) solution was used to back-analyse 4 well-documented field case studies of backfill plug stability – 3 of these for continuous pours and the fourth for a staged backfill with a cure period between the plug and main pours.

A key component of these back-analyses was a comprehensive data review of the strength gain with curing time, obtained from controlled laboratory tests and verified with additional UCS testing data at each mine site during the pours. The authors have continued to use the suggested method to good effect and are aware of others using the method in practical mine design. However, to our knowledge no further case studies have been conducted to either verify the sufficiency of the method or to suggest any optimisation of it. The authors have, however, applied the method to cases where at least some of the original material property or geometric assumptions were not strictly adhered to, and the insights gained may be useful to others. Hence, the purpose of this paper is to address some of the original restrictions of the method and suggest how the method may be applied more broadly. First, however, the most important aspects of the original analysis are reviewed to identify the restrictions for further consideration.

2 Background to the Grabinsky et al. (2021) analysis method

The plug strength method was developed originally to define theoretical paste strength requirements adequate to enable a continuous pour, such that a balance between increasing strength in the plug and the increasing load induced by the main pour could be defined. To our knowledge the method has not yet been used for this 'continuous pour' purpose in design, with the noted case study calibrations being performed retroactively. As a note of caution, the need for instrumentation to verify assumptions was strongly recommended in Grabinsky et al. (2021), as is a generally conservative approach to continuous pouring (Thompson et al. 2023).

Despite the 'continuous pour' element of the original paper, the plug strength method was in fact motivated by the realisation that although barricade designs typically assume fluid loading equivalent to a limited height above the brow, there was no rational engineering approach to define the plug strength required to realise this assumption. Practically, the method is extremely useful in defining plug strength during a two-stage pour, by assuming a plug strength requirement adequate to support the full main pour height. This is in fact a reasonable assumption as 'low binder' main pour pastes at Kidd and Çayeli mines were shown to remain in a hydrostatic state for 24–48 hours (Thompson et al. 2011, 2012). The defined plug strength is required prior to the onset of the main pour, and represents the average plug strength, i.e. the paste strength at the mid-height of the plug should achieve the target UCS prior to the onset of main filling.

Worked examples were provided by the authors in the Australian Centre for Geomechanics' 2025 *Comprehensive Handbook on Minefill* (Potvin et al. 2025), with a 40 m height stope requiring a 207 kPa UCS, which is reasonably consistent with the original 2005 ACG recommendation. For taller stopes (inherently requiring higher UCS), it could be considered that neglecting continued strength gain in the plug (and incremental strength gain in the main) is overly conservative. That, however, would tend to be an extremely site-specific consideration that is outside the scope of this paper to examine.

The parameterised geometry for the original 2021 plug strength analysis method is shown in Figure 1 and the corresponding semi-analytic solution for the required cohesion, c , is given in Equation 1. It is assumed that the undercut cross-section is square (i.e. the out-of-plane undercut width is equal to the undercut height, H_u). This is generally a reasonable assumption, although there are cases where the width significantly

exceeds the height (i.e. width up to twice the height has been encountered by the authors). The setback from the undercut brow to the barricade is L_u , and many operations have requirements for a minimum setback (often $L_u = 1.5 \times H_u$) to protect workers from potential bounce-back of rock falling into the open stope. Some mines also require a safety berm to be constructed under the brow as an additional measure of protection. In contrast, some operations use a 'push-in' type barricade where the initial falsework is constructed on a frame and then advanced very close to the brow resulting in, effectively, $L_u = 0$. Aside from this practice being inherently riskier and resulting in an impractically high UCS requirement when L_u tends to zero, numerical modelling indicates that a different plug failure mechanism may form for the $L_u = 0$ case. Therefore, the plug strength method should not be used with push-in barricades located very near the brow.

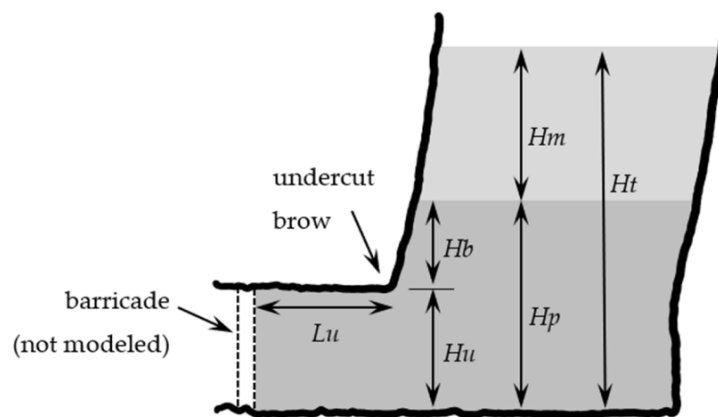


Figure 1 Geometric assumptions for the Grabinsky et al. (2021) plug strength analysis

$$\gamma(H_m + H_b + 0.55H_u) = c \left(\frac{4H_b}{H_u} + 3 + \frac{4L_u}{H_u} \right) \quad (1)$$

The total plug height, H_p , is comprised of the undercut height and the plug height above the brow, H_b . An implicit assumption was that the stope wall above the brow is sub-vertical; however, there are some mine geometries for which the surface is much flatter. It needs to be investigated if the undercut slowly increasing into the stope will lead to greater plug resistance. Also, the original method assumed the undercut would have a square cross-section, but there are many cases in practice where the undercut widens out proximate to the stope, and so the implications of wide undercuts need to be considered.

The method was originally intended to be used with stope designs that employ shotcrete (arched) barricades. It was assumed a worse-case plug fluid backfill pressure distribution arising from an uncured plug pour could bring the barricade to near failure, in which case the structure could not sustain any further deformation arising from the main pour acting on the plug. Therefore, the resistance arising from the shotcrete barricade was not included in the analysis. However, where waste rock berms (WRBs) are used, this assumption is unduly restrictive, and so the application of the method to WRBs needs to be considered.

The previously referred to field studies (namely, Thompson et al. 2011, 2012) investigated cemented paste backfill (CPB) and demonstrated through field monitoring that the total pressure was equal to porewater pressure for many hours during filling. This indicates a state of zero effective stress and implies the paste must behave in the undrained state. In the original paper, 2 concerns were raised: 1) the justification for the assumption that undrained shear strength = $\frac{1}{2}$ UCS had not been adequately demonstrated in the literature (even though this is a common assumption); and 2) that the drainage conditions at the undercut's bottom surface could result in a drained backfill layer overlain by the remaining undrained backfill. Recent developments (Grabinsky et al. 2025 2026) indicate that this material behaviour assumption needs to be reassessed.

Where backfilling is carried out using cemented hydraulic fill, the intermittent nature of the filling method means that the backfill is more likely to behave in the drained state and therefore the influence of backfill friction angle should be considered.

The effects of the mentioned new parameters are considered in the remainder of this paper.

3 Effect of transitional undercut geometries into the stope

Figure 2 shows an example arising from a representative orebody geometry where the immediate hanging wall is inclined at a shallow angle (as shown, rise-run is 3:4) before reaching the main stope. It was initially thought this might be a more stable situation compared to the geometry shown in Figure 1, as plug failure would involve a larger backfill mass through the narrowing portion from the stope towards the undercut. Analyses were therefore carried out to test this hypothesis. Results are shown in Figure 3 for both modified and conventional geometries.

Nonlinear analyses were carried out using RS3 from Rocscience. The analyses were run assuming a 160 kPa pressure on the plug's top surface and reducing the backfill cohesion iteratively until large strains, displacements and numerical non-convergence occurred. Surprisingly, the limiting undrained shear strength was virtually identical. The contour patterns in Figure 3 suggest the failure mechanism is slightly different (to be expected based on the different geometric boundary condition). A similar analysis was run with a taller plug and again the difference between modified and conventional geometries did not impact the numerically determined limiting undrained shear strength. It remains to be determined if there is a satisfactory theoretical explanation for this finding, for example by using limiting equilibrium models with failure geometries motivated by the failure mechanisms suggested by the numerical analyses.

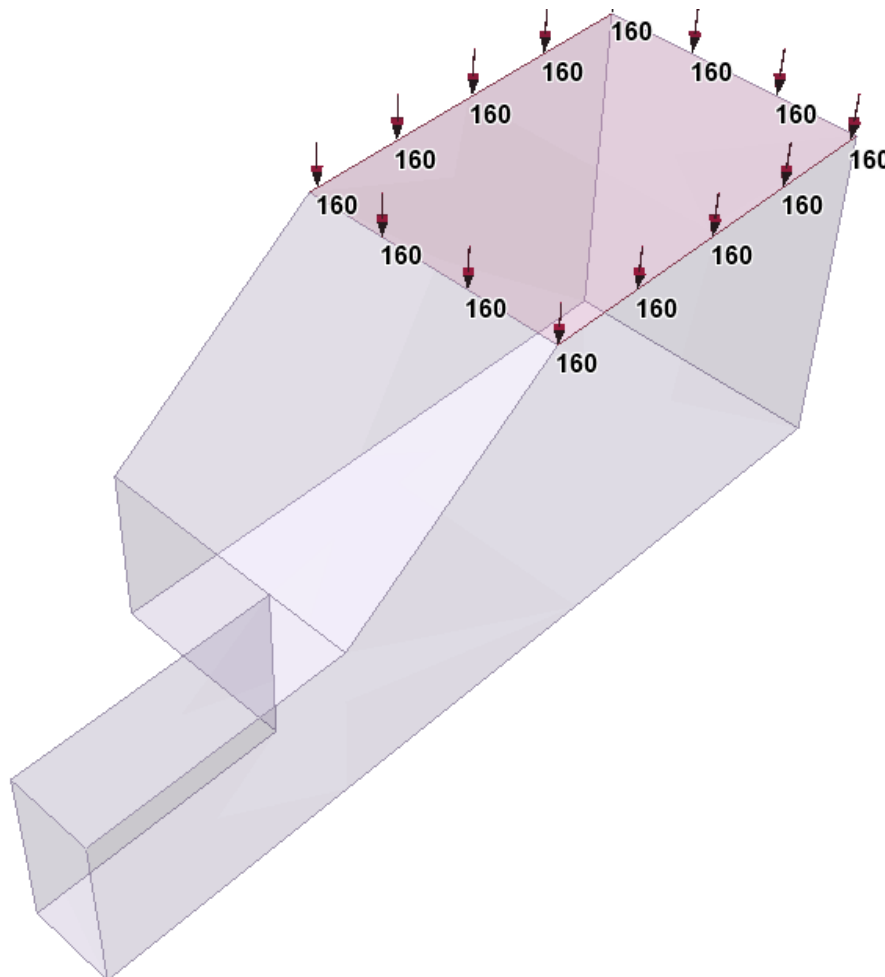


Figure 2 Example of transitional geometry between undercut and main stope

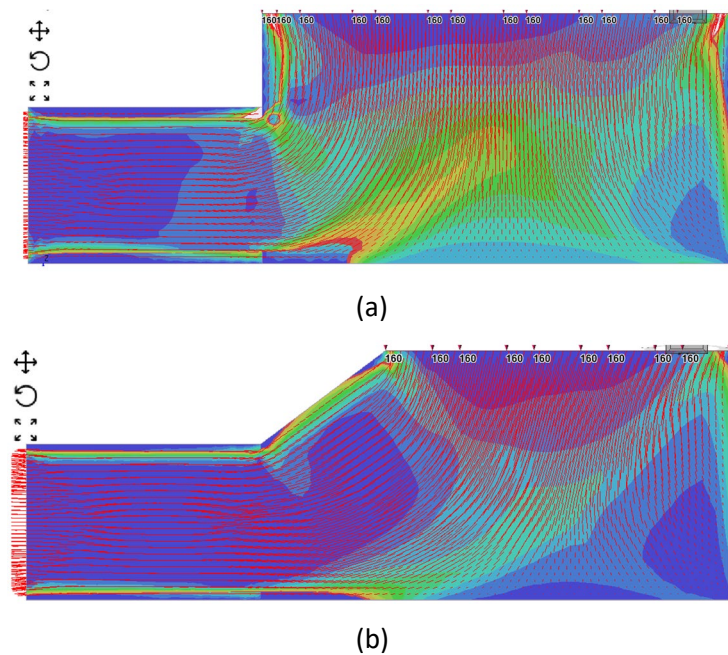


Figure 3 Numerical results for the (a) conventional geometry compared with (b) the modified geometry. Contours are maximum shear strain (from low [blue] to high [red]) and the red arrows show deformation pattern

4 Effect of non-square undercut cross-sections

The Skempton (1951) adaptation of Prandtl's solution for shallow foundations assumed the minimum footing width is B and the longest dimension is L . The Prandtl solution was presented for a two-dimensional analysis (i.e. $L \rightarrow \infty$, applicable to strip footings) and Skempton suggested the shape factor for finite (rectangular or square spread footings) should be $(1 + 0.2 B/L)$. Therefore, a square spread footing can sustain a 20% higher applied pressure than a strip footing of the same width. How might this apply to non-square undercut geometries?

Figure 4 shows the assumed plug failure mechanism, which is consistent with the mechanism observed from numerical analyses of identical slope and undercut geometries. The $\frac{1}{2}$ Prandtl mechanism consists of zones 2 and 3 in Figure 4. Zone 2 is the passive wedge (horizontal stresses are higher than vertical stresses) and zone 3 is a 'fan failure' zone where the orientation of the principal stresses rotates and the major compressive stress decreases ongoing from zone 2 to zone 4. From the geometric construction shown in Figure 4, the extent of the failure mechanism into the slope equals $\sqrt{2}H_u$, or about $1.4H_u$. However, if the undercut cross-section is square, then the out-of-plane dimension of the failure mechanism is H_u , meaning the equivalent 'footing' has dimensions $\sqrt{2}H_u$ in-plane and H_u out-of-plane, which violates the original Skempton (1951) assumption that the in-plane dimension is the shortest. This is why one of the terms in the original semi-analytic solution (the effective weight of the $\frac{1}{2}$ Prandtl wedge) had to be numerically calibrated.

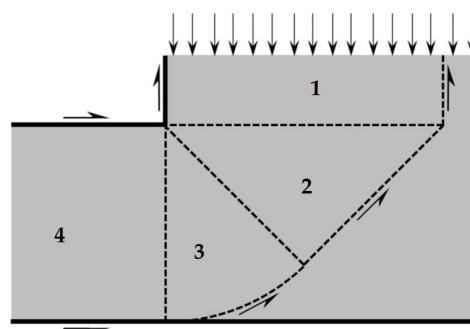


Figure 4 Assumed failure mechanism for plug analysis

To better understand the effect of the undercut's out-of-plane width, W_u , the original solution (which assumes $W_u = H_u$) was compared with 2D analyses using the same in-plane geometry (and therefore represents the ' $W_u \rightarrow \infty$ ' extreme case) and various 3D analyses with square and non-square undercut cross-sections. The modelled undercut height is $H_u = 5$ m and the modelled plug height is the same as the undercut height; therefore, the height of the plug above the brow $H_b = 0$. Applied surcharges of 100 and 200 kPa (representing 5 and 10 m of main fill with 20 kN/m^3 unit weight, respectively) were modelled. The modelled length of the undercut $L_u = 5$ m. The theoretical solution predicts a limiting cohesive strength of 22 kPa for the 100 kPa surcharge, and 36 kPa for the 200 kPa surcharge. Modelling results are shown in Figure 5, and the 2D solution is approximately 50% greater than the proposed analytic solution. Note that the cohesion values shown in Figure 5 are for the limiting case, i.e. strength factor (SF) = 1. A shape function like Skempton's was fit to the data, then inverted so that it could be applied to Equation 1. Therefore, for non-square undercuts, the limiting cohesion can be found from (Equation 1) $\times 1.5/(1 + H_u/2W_u)$. Note that this is a somewhat stronger shape factor than was originally proposed for the Skempton (1951) solution.

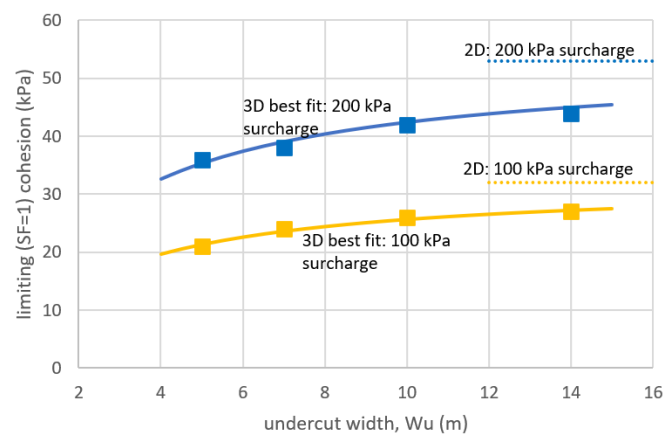


Figure 5 Effect of non-square undercut cross-sectional dimensions (modelled undercut height $H_u = 5$, out-of-plane undercut width is W_u). Cohesions are for the limiting condition (strength factor, $SF = 1$)

5 Plug design for waste rock berms

Typically, a WRB is constructed with the WRB's slope-side crest-back contact significantly closer to the slope brow than occurs with barricades (for which typically $L_u = 1.5 H_u$). Practically, application of Equation 1 to a WRB is therefore problematic given the potentially high UCS requirement resulting from small L_u values. As noted earlier, numerical analysis shows, in fact, the failure mechanism of the plug may change as L_u tends to zero, and so theoretically, application of Equation 1 to plug design in conjunction with WRB use is problematic, and so not recommended.

A fundamental contrast between the function of the plug to isolate a barricade compared to isolating a WRB, is that theoretically a barricade may suffer deformation during initial fluid plug loading, such that continued loading during a main pour could induce barricade failure. It is for this reason that contribution of barricade strength is neglected in the plug strength formulation. In contrast, however, WRBs are massive structures that easily accommodate the relatively small, continued deformations during main pour loading. It is less clear, therefore, if the plug must isolate the WRB from additional loading by the main pour, or if a more nuanced design is feasible whereby the WRB and plug provide combined resistance.

To consider an alternative plug strength requirement for use with WRB containment, it is first necessary to review design assumptions, as follows. In an analytical solution for the stability of WRBs, Zhai (2022) demonstrates that realistic WRB geometries and material properties imply that 'global' failure involving block shear along the sidewall and floor contact with rigid body movement of the WRB along the drift axis is a virtual impossibility. Instead, a 'local' failure involving shearing through the WRB's top surface will invariably control design.

To enable discussion in the context of plug strength design, generic analysis results in Figure 6 illustrate such a mechanism formed during numerical analysis for a WRB. The backfill in the main stope is assumed to impose a fluid head on the WRB's stope-side face (a worst-case loading assumption). When the backfill in the main stope is X m high (Figure 6a), strain localisation near the WRB's top is evident from the discontinuous and irregular total displacement patterns. When the fill is $X + 1$ m high (Figure 6b) the displacement localisation is accentuated and the kinematically feasible sliding block shearing through the WRB's top surface is clearly visible. Note, dimensions of X and $X + 1$ are used as it is outside the scope to comment on WRB strength. The key aspect of analysis is to emphasise that displacement has accelerated quickly within a 1 m loading increment.

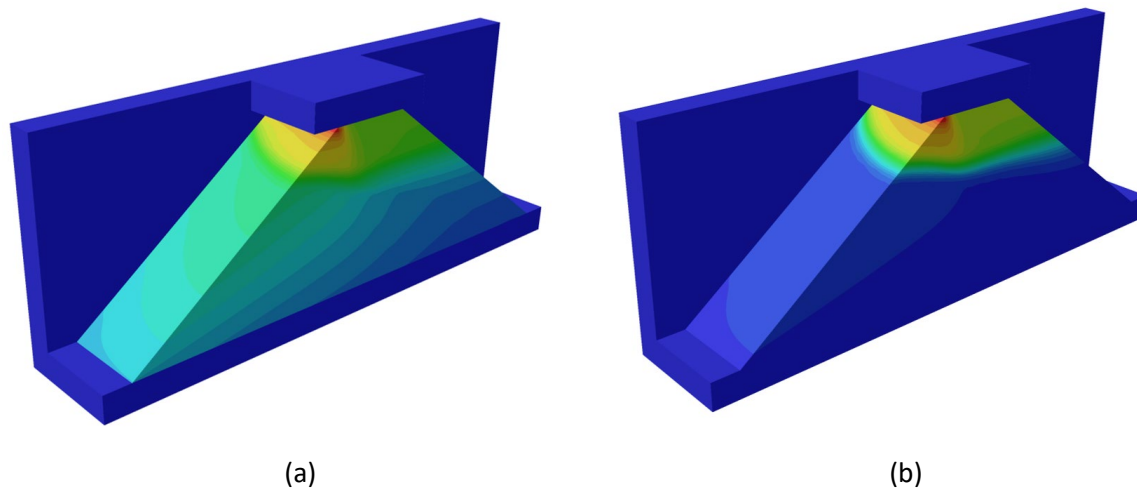


Figure 6 Numerical results for an analysed waste rock berm when the stope backfill is (a) X m above the floor and (b) $X + 1$ m above the floor. Contours are total displacement from zero (blue) to maximum (red), and the maximum displacement is (a) 5 cm and (b) 35 cm

For a WRB to behave as the idealisations in Figure 6 suggest, attention must be paid to quality construction practices. Particle size segregation during waste rock placement must be avoided and proper compaction of each waste rock layer must be achieved. This is particularly critical at the WRB's contact between the WRB at the top (roof, or back) of the undercut. Gélinas (2017), however, indicates heterogeneity (in terms of material size, material properties, and extent of compaction) can be expected in WRB construction. Uncertainty exists with the as-built WRB-back crest length, even for operations with rigorous QA/QC inspection requirements. A recent example described to the authors was a WRB requiring a 6 m crest contact length was found to have only 3.5 m contact length, significantly less than design assumptions. It can be difficult to visually confirm an appropriate contact is established during construction. Further, the extent of paste penetration into the WRB can vary on a site-specific basis. For these reasons, a continuous pour is not recommended, not least because conventional design does not explicitly consider seepage potential along the heterogeneous top contact, or penetration of paste into the WRB. It is conceivable that increasing head pressure arising from the main pour would result in internal erosion type failure of the WRB if plug strength is inadequate. It is therefore recommended that a plug pour and plug cure period be used with a WRB.

A second design requirement for a paste plug used in conjunction with a WRB is to achieve sufficient strength to be liquefaction resistant. Although uncertainty with current definition of a correspondingly suitable UCS is discussed in Grabinsky et al. (2026), limitations with practically determining UCS accurately at low strengths justifies a conservative approach.

While penetration of paste into a WRB poses an initial concern, the presence of paste will presumably increase WRB strength if it has reached a state of initial set. This provides additional conservatism to WRB design if it is assumed a paste plug has adequately cured. The plug-WRB system is relatively complex and so beyond the scope of this work to recommend a definitive design solution. Site-specific considerations must be carefully assessed by a practitioner, with additional conservatism warranted by limitations in WRB

construction QA/QC, potential variation in paste mixtures and performance, difficulties with monitoring pressures acting upon WRBs, and the consequences of failure.

6 Effect of friction for cemented hydraulic backfills

The frictional effects of backfill were investigated using 2D models with $H_u = L_u = 5$ m, $H_b = 0$, and $H_m = 10$ m, which is the same model described in Section 4 (undercut cross-sectional effects). For the purely cohesive model ($\phi = 0$) the limiting cohesion is 56 kPa as shown in Figure 5, which then implies a required limiting UCS = 112 kPa. Maximum shear strain results for that analysis (not shown here) demonstrate shear localisation and a failure mechanism forming virtually identical to the idealised solution shown in Figure 4.

Subsequent analyses then increase the friction angle and determine the corresponding limiting cohesion and UCS values. Results are shown in Figure 7 in terms of maximum shear strain. As the friction angle increases, the passive wedge (zone 2 in Figure 4) narrows and becomes smaller, and the ‘fan failure’ zone (zone 3 in Figure 4) transitions from a circular arc to a log spiral. These observations are consistent with numerical analyses on shallow foundations as the friction angle increases from zero (the cohesion-only case considered by Skempton).

The limiting values from the numerical analyses are 35 kPa cohesion and 83 kPa UCS for $\phi = 10^\circ$, and 20 kPa cohesion and 57 kPa UCS for $\phi = 20^\circ$ (note that the calculation for UCS accounts for changing cohesion as well as friction angle). Therefore, the UCS required for $\phi = 20^\circ$ is virtually half that required when the material is modelled as pure cohesive ($\phi = 0$). This result indicates that cemented backfill plugs in drained hydraulic fill exhibit remarkable stability, and even if the backfill is in a partially drained state, the lower total friction angle contributes significantly to plug strength.

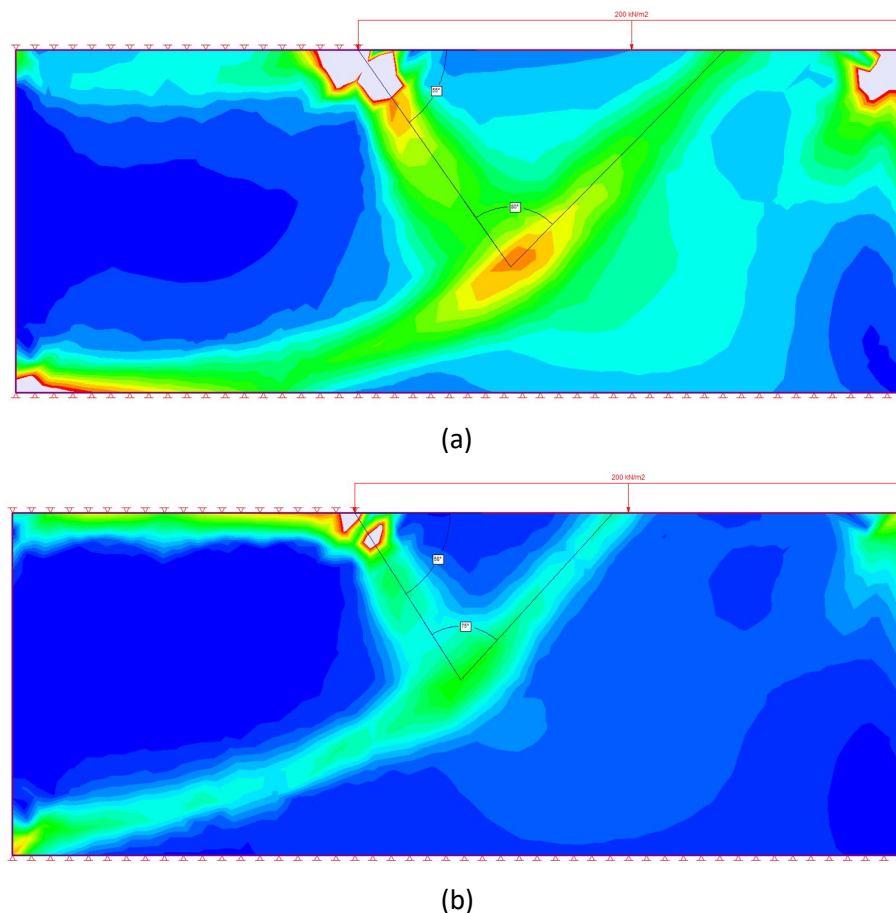


Figure 7 Numerical results demonstrating the stabilising effect of material friction. Total stress friction angle is (a) $\phi = 10^\circ$ and (b) $\phi = 20^\circ$. Contours are maximum shear strain, from zero (blue) to maximum (red)

7 Effect of undrained cemented paste backfill material properties

A reinterpretation of published data using undrained triaxial testing with porewater pressure measurements on cemented paste backfill with strengths in the range ~200 kPa to just over 1 MPa UCS is presented by Grabinsky et al. (2025, 2026). The results from total stress analyses were presented in a normalised form by dividing both the shear and normal stresses by the material's UCS. The results are reproduced in Figure 8. The shear stress is expressed as $t = \frac{1}{2}(\sigma_1 - \sigma_3)$ and the normal stress is expressed as $s = \frac{1}{2}(\sigma_1 + \sigma_3)$, and any s-t point in this space represents the top of an equivalent Mohr's circle for the corresponding principal stresses.

The failure envelopes for each of the control UCS values are shown only between the limits obtained from the tests conducted at confining pressures about 100, 200, 300 and 400 kPa. Therefore, the failure envelope for the UCS = 307 kPa test series appears to be longer than for the UCS = 1,276 kPa test series as shown in the normalised stress space. Also on this figure is the theoretical stress path for a UCS test, rising from the origin at a 45° angle and terminating at (0.5, 0.5). Note that the total stress failure envelopes can be reasonably extrapolated back to the theoretical UCS point (shown as a red dot), or slightly above it. Therefore, it is reasonable to assume the undrained cohesion = $\frac{1}{2}$ UCS. The results in Figure 8 and the interpretation arising from it are arguably the strongest justification yet for the commonly used heuristic for backfill's undrained shear strength. Furthermore, when conducting total stress analyses, it is reasonable to assume that a modest total stress friction angle also exists, at least 10° from the results shown in Figure 8.

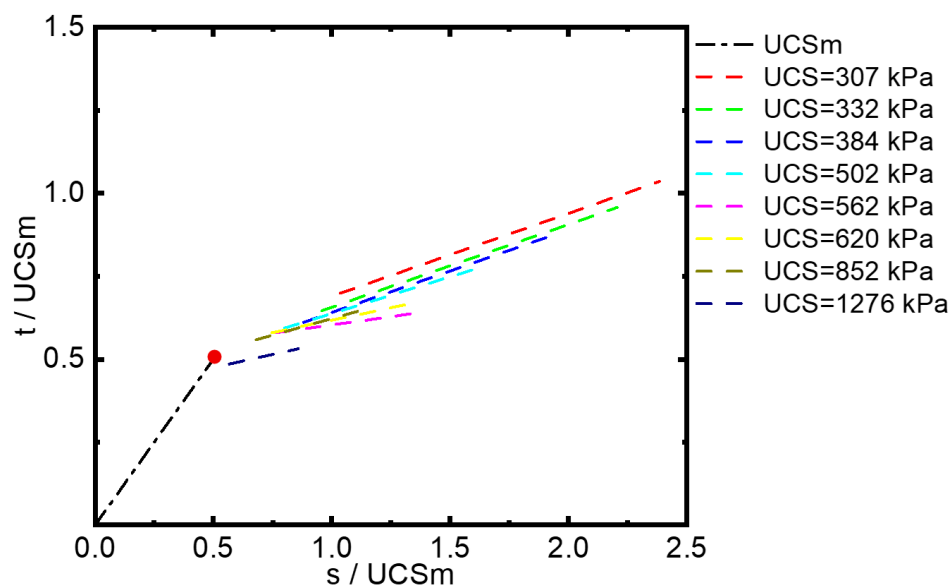


Figure 8 Total stress failure envelopes (shown only within the limits of the confining pressures used for testing) and theoretical stress path for a UCS test, terminating at (0.5, 0.5) or $\frac{1}{2}$ UCS

Note from the previous section that even a 10° total stress friction angle can result in a significant reduction in the required UCS (83 versus 112 kPa in the given example, or a 26% reduction). However, it is probably best to use the original equation (Equation 1) as is with the understanding that any undrained friction acting in the material results in an inherent factor of safety or strength factor.

If Equation 1 is used to compute the required cohesion, then the UCS should be determined as twice this value. The original paper assumed that the UCS should be 4c based on an assumed friction angle 37° and drained behaviour along the base of the undercut, assuming only the cohesive component of the drained material could be mobilised. However, if instead the UCS = 2c assumption is used, yet the hypothesised drained base condition exists, will the design still be safe?

Figure 9 shows the original figure proposed to estimate the limiting strength for the plug to be self-supporting (i.e. as though the barricade could be removed, and the plug would remain stable). If the above argument means the recommended strengths can be halved, then the required plug strength will always be less than

$0.4\gamma H_u$. Considering the construction of a Mohr's circle with a total stress failure envelope for $\phi = 0$ tangent to the top of the circle for the undrained case, versus an effective stress failure envelope tangent to the Mohr's circle with intercept $\frac{1}{2}c$ and friction angle 37° , the same shear resistance will be mobilised in effective stress as would be in total stress when the normal stress is $\frac{1}{2}c$, or at most $\frac{1}{3}(0.4\gamma H_u) \approx 0.27\gamma H_u$. However, the normal stress will be the plug's self-weight effect, γH_u . Therefore, the undrained condition will always dominate the strength requirement. Even if the bottom layer of the plug is drained and can therefore support more shear stress, the critical failure surface will lie just above this drained layer, through the remaining undrained backfill material. It is therefore safe to continue using Equation 1 to calculate the limiting (SF = 1) cohesion but now determine the limiting UCS as twice this value. It should also be noted that this new interpretation does not change the findings of the case studies presented in the original paper. The analyses for Cayeli 685, Williams and Kidd would still show a viable continuous pour (but with greater SFs), and the Cayeli 715 analysis would still show that the cure period between the plug and main pours was required.

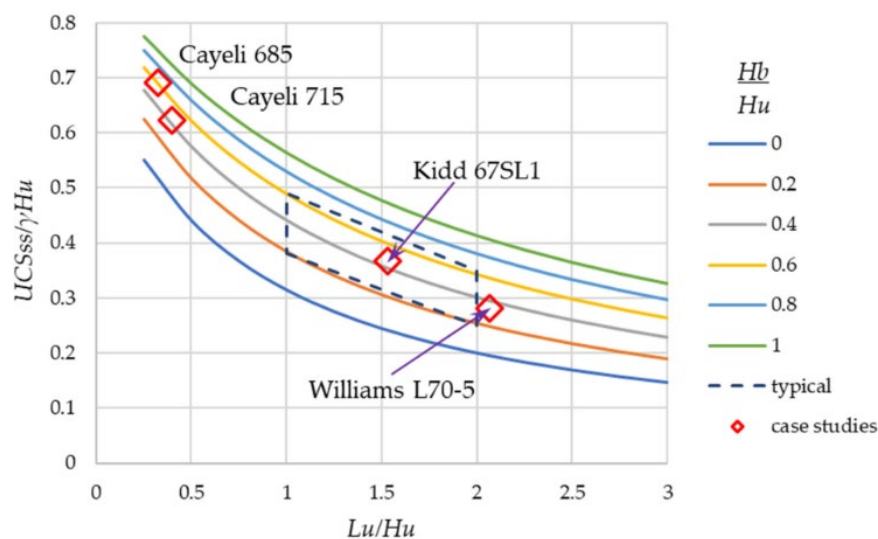


Figure 9 Strength requirement for self-supporting plug strength, UCS (reproduced from Grabinsky et al. 2021) based on the assumption $UCS = 4c$. If $UCS = 2c$, then the values determined from this figure have a strength factor = 2.0

8 Practical application and strength factors

This paper has presented significant reinterpretation of how Grabinsky et al.'s plug strength method may be applied. In particular, the change to definition of UCS based on $2c$ rather than $4c$, has implications that require careful consideration.

The authors have previously applied the method for design purposes without adding a strength factor, given appreciation of inherent conservatism (as described, with definition of cohesion, and the earlier described assumption of requiring plug strength sufficient to support the full stope height, prior to the start of the main pour). Confidence in the original application of the method (with $UCS = 4c$) was also provided by the realisation that the strength required typically exceeded the original Potvin et al. (2005) 150 kPa recommendation, for which there is arguably a measure of empirical validation. Finally, an explicit recommendation of monitoring barricade pressures to validate loading assumptions has provided additional confidence in application of the plug strength method.

This paper has presented rationale to better understand some of the 'inherent conservatism' of the original method. It is important to recognise that incorporation of the identified improvements reduces the extent of inherent conservatism, with the updated edition more closely representing a limiting condition. It is therefore necessary to put equal focus on definition of a suitable SF. As an inherent part of the backfill containment system, plug design does warrant a conservative approach as the consequences of barricade

failure presents risk of fatalities. To this end, $SF = 2$ is recommended for design, although site-specific assessment is always required.

From a practical perspective, relatively few mines conduct early age paste UCS testing (i.e. 1–3 days' curing). Publication of case studies presenting early age paste UCS data correlated with barricade pressure data would be extremely beneficial, potentially providing important validation of, or additional insights into, plug strength design.

9 Summary and conclusion

The plug and main pour concept of backfill placement represents a key component of the backfill containment system, and this paper has provided a reinterpretation of an original method for calculating the plug strength requirement. The proposed improvements have been developed in part as a response to operational applications where implementation required revision, or re-assessment of original assumptions and variables. Key updates are described below.

The most significant difference between the original and updated application is with the recommendation to use Equation 1 to calculate the limiting cohesion and then calculate the limiting $UCS = 2c$, rather than the originally proposed $UCS = 4c$.

Notably, this and other changes reduce inherent conservatism previously identified, and so it is necessary to apply an SF to the plug strength calculation, where an $SF = 2$ is reasonable given the consequences of containment failure.

Limitations have been identified if applications require a reduced value of Lu , in comparison to the conventionally assumed $Lu = 1.5 Hu$. Specifically, the method should not be used for 'push-in' barricades where Lu approaches zero.

It is not recommended that the plug strength method be used for WRBs. Instead, the plug design should ensure adequate cure time to achieve an initial paste set, reduce hydraulic conductivity, prevent paste seepage, and to satisfy the relevant liquefaction resistance criteria.

Stress analyses incorporating effective stress (drained) friction angles show dramatic improvement in stability, and reduced extent of the formed failure mechanism. Cemented backfill plugs for hydraulic fill should therefore be expected to be very stable and may require a relatively low plug strength in comparison to paste plugs.

Non-square undercut cross-sections, with undercut width Wu exceeding undercut height Hu , do require increased plug strength. It is recommended that Equation 1 be used with a shape factor $1.5/(1 + Hu/2Wu)$. This means the plug strength would have to be increased by at most 50% in the limit $Wu \rightarrow \infty$, which is clearly a very theoretical upper bound.

Transitional geometries of the type shown in Figure 2, although rare, do not require changes to the plug strength calculation method. The reasons for this are not clear and require further investigation for a detailed explanation, although this is not of practical significance.

The original application of the method resulted in UCS requirements that typically exceeded conventionally assumed liquefaction resistance and bond crushing limits. As perhaps can be expected for hydraulic fills, if friction angle is included in a plug strength assessment, design recommendations must now also consider these alternative design metrics.

As consistent with recommendations from Grabinsky et al. (2021), the theoretical framework of the approach should be acknowledged and verified with cautious application and a requirement for pressure monitoring to verify assumptions and ensure pressure thresholds are not exceeded. An expanded database of mine site early age paste plug UCS correlated with measured barricade pressures would be useful to better understand and calibrate the response of the barricade–plug strength containment system.

Acknowledgement

The authors gratefully acknowledge the informative discussions with colleagues and industry partners who have provided the motivation to conduct this work. The thoughtful recommendations from the 2 anonymous reviewers are also appreciated.

References

- Gélinas, L-P 2017, *Caractérisation des Propriétés Géomécaniques des Barricades Rocheuses et des Chantiers Miniers Remblayés en vue de leur Analyse de Stabilité (Characterisation of the Geomechanical Properties of Rock Barricades and Backfilled Mining Workings with a View to Their Stability Analysis)*, master's thesis, École Polytechnique de Montréal, Montréal, www.publications.polymtl.ca/2957/
- Grabinsky, M, Bawden, W & Thompson, B 2021, 'Required plug strength for continuously poured cemented paste backfill in longhole stopes', *Mining*, vol. 1, pp. 80–99, <https://doi.org/10.3390/mining1010006>
- Grabinsky, M, Jafari, M, Thompson B & Veenstra, R 2025, 'A framework for understanding static liquefaction of tailings with cohesion: insights from cemented backfill', in GW Wilson, DC Sego & J Goodwill (eds), *Proceedings of the Tailings & Mine Waste Conference 2025*, University of Alberta, Edmonton, pp. 1451–1460, <https://tailingsandminewaste.com/conference-proceedings/>
- Grabinsky, M, Jafari, M, Thompson, B & Veenstra, R 2026, 'Interpreting laboratory liquefaction test results: the importance of confining pressure to unconfined compressive strength ratios', in AB Fourie, M Horta, M Oliveira & S Wilson (eds), *Paste 2026: Proceedings of the 28th International Conference on Paste, Thickened and Filtered Tailings*, Australian Centre for Geomechanics, Perth, https://doi.org/10.36487/ACG_repo/2655_15
- Potvin, Y, Thomas, E & Fourie, A (eds) 2005, *Handbook on Mine Fill*, Australian Centre for Geomechanics, Perth.
- Potvin, Y & Veenstra, R (eds) 2025 *Comprehensive Handbook on Minefill*, Australian Centre for Geomechanics, Perth.
- Skempton, AW 1951 'The bearing capacity of clays', *Proceedings of the Building Research Congress*, Institution of Civil Engineers, London, pp. 180–189.
- Thompson, B, Grabinsky, M & Bawden, W 2011, 'In situ monitoring of cemented paste backfill pressure to increase backfilling efficiency', *CIM Journal*, vol. 2, pp. 199–209
- Thompson, B, Bawden, WF & Grabinsky, M 2012, 'In situ measurements of cemented paste backfill at the Cayeli Mine', *Canadian Geotechnical Journal*, vol. 49, pp. 755–772
- Thompson, BD, Veenstra, RL, Carmichael, P, Bawden, WF & Grabinsky, MW 2023, 'Best practices in continuously (or not continuously) pouring paste backfill', in GW Wilson, NA Beier, DC Sego, AB Fourie & D Reid (eds), *Paste 2023: Proceedings of the 25th International Conference on Paste, Thickened and Filtered Tailings*, Australian Centre for Geomechanics, Perth, pp. 279–293, https://doi.org/10.36487/ACG_repo/2355_21
- Zhai, Y 2022, 'An update of the 3D analytical solution for the design of barricades made of waste rocks', *International Journal Rock Mechanics & Mining Sciences*, vol. 158, <https://doi.org/10.1016/j.ijrmms.2022.105176>